Journal of Chromatography B 1227 (2023) 123838

Contents lists available at ScienceDirect

Journal of Chromatography B

journal homepage: www.elsevier.com/locate/jchromb

IgG glycomic profiling identifies potential biomarkers for diagnosis of echinococcosis

Xiaoxiao Feng [b,1], BaiMaYangJin [a,1], Xiaojin Mo [c], Fangyan Zhang [d], Wei Hu [c], Zheng Feng [c], Ting Zhang [a,c,*], Liming Wei [b,*], Haojie Lu [b,*]

[a] National Health Commission Key Laboratory of Echinococcosis Prevention and Control, Xizang Center for Disease Control and Prevention, Lhasa 850000, Tibet Autonomous Region, People's Republic of China
[b] The Fifth People's Hospital of Shanghai, Institutes of Biomedical Sciences, Shanghai Cancer Center, Department of Chemistry & NHC Key Laboratory of Glycoconjugates Research, Fudan University, Shanghai 200032, People's Republic of China
[c] National Institute of Parasitic Diseases, Chinese Center for Disease Control and Prevention (Chinese Center for Tropical Diseases Research), NHC Key Laboratory of Parasite and Vector Biology, WHO Collaborating Center for Tropical Diseases, National Center for International Research on Tropical Diseases, Shanghai 200025, People's Republic of China
[d] Waters Technologies, Pudong New District, Shanghai 201203, People's Republic of China

ARTICLE INFO

Keywords:
Echinococcosis
Echinococcus
Glycome
Serum
immunoglobulin G (IgG)
Diagnosis

ABSTRACT

Echinococcosis caused by larval stage of the genus *Echinococcus*, is a serious and potentially fatal parasitic zoonosis distributed globally. The two types of the disease in human are cystic echinococcosis (CE) and alveolar echinococcosis (AE). As the biological and encysting characteristics of the parasite, early diagnosis remains to address. In the present study, we demonstrate the value of Immunoglobulin G (IgG) glycome as a potential diagnostic biomarker for echinococcosis. Serum IgG glycome profiles were analyzed by ultra-performance liquid chromatography in a cohort comprised of 127 echinococcosis patients, of them 98 were diagnosed as CE and 29 as AE. IgG N-glycome analysis in pretreatment serum of echinococcosis patients presents 25 glycans and 64 derived traits. Compared with IgG glycans of healthy control group, neutral glycans, fucosylation and agalactosylated N-glycans increased while sialylation and galactosylation decreased in echinococcosis patients. Combined with a machine-learning-based approach, we built three biomarker combinations to distinguish CE, AE and healthy controls. Meanwhile, galactosylation, sialylation and A2BG2S1 in IgG glycan profiles were evidently associated with different types of CE (from CE1 to CE5). Our findings suggest that the alterations in IgG N-glycome may be of value in CE and AE diagnosis and follow-up CE disease progress. The role of IgG N-glycans as diagnostic biomarker remains to be verified in future study.

1. Introduction

Echinococcosis, a parasitic zoonosis, caused by the larval stage of the genus *Echinococcus* [1–5]. More than 1 million people are affected with echinococcosis at any one time, and humans are infected through ingestion of parasite eggs in contaminated food, water or soil, or after direct contact with animal hosts [6,7]. Echinococcosis is often expensive and complicated to treat and may require extensive surgery and/or prolonged drug therapy. The two major species that infect humans are *E granulosus* and *E multilocularis*, which cause cystic echinococcosis (CE) and alveolar echinococcosis (AE). This zoonosis is characterised by long term growth of metacestode cysts in humans and mammalian intermediate hosts [2,8–10]. CE is the most prevalent form of echinococcosis in humans, accounting for about 70% of the total cases, causing serious health impairments and significant economic burden globally [11,12]. AE occurs in the northern hemisphere and imposes a higher disease burden than CE because of its high fatality if managed untimely and inadequately [13,14]. The WHO-IWGE expert consensus has been reached that ultrasound (US) examination is the basis of CE and AE diagnosis in abdominal locations. Based on US imaging, hepatic CE cysts are classified into six types of CL (cystic lesion) and CE1 to CE5, according to the cyst activity, while AE lesions into different PNM (parasite

* Corresponding authors at: The Fifth People's Hospital of Shanghai, Institutes of Biomedical Sciences, Shanghai Cancer Center, Department of Chemistry & NHC Key Laboratory of Glycoconjugates Research, Fudan University, Shanghai 200032, People's Republic of China (H. Lu).
E-mail addresses: zhangting@nipd.chinacdc.cn (T. Zhang), weiliming@fudan.edu.cn (L. Wei), luhaojie@fudan.edu.cn (H. Lu).
[1] These authors contributed equally to this work.

https://doi.org/10.1016/j.jchromb.2023.123838
Received 1 February 2023; Received in revised form 25 June 2023; Accepted 18 July 2023
Available online 25 July 2023

lesion, neighbor organs, metastases) types [15]. Though it has been widely applied clinically, the challenge in imaging diagnosis of echinococcosis is detecting small cysts/lesions (<2 cm in diameter) [16]. Serological detection plays an important complementary role in confirming imaging results, and following-up after surgery or chemotherapy.

The variation and severity of clinical expression of disease may mirror the host's immunological responses to the parasite [17]. Early diagnosis of echinococcosis may provide information for early treatment and more effective chemotherapy, however, it is difficult due to the typical asymptomatic features in the early stages of infection, and physical imaging usually used in the late stages of infection [18]. It is believed that the host's immunological response could be the earliest detection indicator after infection. Immunoglobulin G (IgG), a highly abundant glycoprotein in serum, is known to be one of the most important glycoproteins in the immune system [19,20]. The earliest IgG response to CE hydatid cyst fluid and oncospheral antigens occurred after a few weeks in animal study [18]. Due to the diverse clinical manifestations of hydatid cysts, each type of hydatid cyst has different growth and reproduction features, causing differences in host immune responses, which poses challenges to accurate diagnosis, and to a certain extent, contributes to the instability of sensitivity and specificity in antibody IgG detection. Moreover, there is no applicable diagnostic biomarkers available for differentiation of CE and AE, despite of antigen Em18 showed the potential in the discrimination [21]. Thus, identification of serum immunological markers for diagnosis of echinococcosis draws increasing concern.

Glycosylation, which is a common and complex post-translational modification (PTM), participates in and regulates most important biological processes, such as cell adhesion, growth, differentiation, apoptosis, molecular transport, receptor activation, and signal transduction [22–26]. It occurs during antibody synthesis and is essential for both antibody structure and molecular activity. The N-glycosylation profile of IgG exerts a strong influence in immune process and regulatory responses in the host and can profoundly affect the outcome of disease [27–30]. Extensive studies suggested that IgG glycans may act as potential biomarkers of various diseases, such as rheumatoid arthritis, ischemic stroke, dyslipidemia, diabetes, and many cancers [31]. Studies on parasite glycans revealed that schistosomes express a large number of glycans as part of their glycoprotein and glycolipid repertoire, and antibody responses to those glycans are mounted by the infected host [32]. It is noted that sialylated N-glycan in Toxoplasma infection in mice was demonstrated as a novel biomarker of sickness/depressive-like behaviors [33], while collective data indicated that *E. caproni*-expressed glycans play a major role in the modulation of the immune responses [34]. However, the knowledge on Echinococcus glycan is devoid. Given the N-linked glycosylation correlates with parasite-induced immunoregulation, we hypothesized that the IgG glycome profiles of Echinococcus may be of significance for understanding the role of IgG glycans in the disease progress and identifying potential biomarkers for diagnosis. In this study, we applied a fluorescently-based glycomic analysis combined with machine-learning-based approach to profile the glycome of echinococcosis serum IgG, resulting in the potential combinations of IgG glycan peaks and derived traits (IGPs) for the classification of CE, AE cases and healthy controls, and the prognostic accuracy was higher than serum antibody IgG enzyme-linked immunosorbent assay (ELISA). Meanwhile, we further employed this approach to explore the role of IgG glycome as the potential biomarkers related with the clinical stages of CE. Several followed-up CE patients over three years further confirmed the potential marker. These findings highlight the link between IgG N-glycome and the physiopathology of echinococcosis and open new research avenues against infectious diseases.

2. Methods

2.1. Materials and reagents

Ammonium bicarbonate (ABC), dithiothreitol (DTT), iodoacetamide (IAA), 2-aminiobenzamide (2-AB), sodium cyanoborohydride ($NaBH_3CN$), 2-picoline borane and dimethyl sulfoxide (DMSO) and trifluoroacetic acid (TFA) were purchased from Sigma-Aldrich (MO, U.S.A.). Acetonitrile (ACN) and glacial acetic acid was from Merck (Darmstadt, Germany). Protein G agarose spin plate was from ThermoFisher Scientific (MA, U.S.A.). Centrifugal filters with a MWCO of 3 and 10 kDa were purchased from Millipore (MA, U.S.A.). Peptide N-glycosidase F (PNGase F, 500 U/μL) was from New England Biolabs (MA, U.S.A.). Distilled water was purified by Milli-Q system (MA, U.S.A.). All other chemicals and reagents of the best available grade were purchased from Sigma-Aldrich (MO, U.S.A.). The commercial enzyme-linked immunosorbent assay (ELISA) kit was from Haitai Biological Pharmaceuticals Co., Ltd. (Zhuhai, China).

2.2. Sample collection

Serum samples were collected from cystic and alveolar echinococcosis patients in the endemic areas of Tibet Autonomous Region, and Gansu, Sichuan, and Qinghai Province of China. In addition, 22 healthy samples were collected from the First Affiliated Hospital of Guangxi Medical University (Nanning, China) used as negative control. All the control samples were also negative in the Epstein-Barr virus and Fasciolidae. The clinic pathological data of the serum were summarized in Table S1. CE and AE were diagnosed based on the US pathognomonic image and confirmatory serological test, while classification was made according to the conformational features of cysts. The serological test conducted for *Echinococcus* IgG antibody was performed using a commercial enzyme-linked immunosorbent assay (ELISA) kit. All serum samples were stored at −80 ℃ until use.

2.3. Isolation and purification of IgG

IgG was isolated from human serum using protein G agarose spin plates (ThermoFisher Scientific, MA, U.S.A.) according to the manufacturer's protocol. Briefly, the plate was pre-equilibrated with 200 μl binding buffer for each well, and centrifuged to remove the buffer afterwards. 10 μl serum sample 10 μl diluted with 90 μl binding buffer was applied into the well and incubated for 3 h with moderate agitation at 4 ℃, followed by centrifugation for 90 s at 3,000 RCF (relative centrifugal force) to discard the flow-through. The resin on the well was washed with 100 μl binding buffer for three times to remove all unbound non-IgG by centrifuging, discarding the flow-through each time. Subsequently, 50 μl elution buffer was added into the well and incubated for 5 min with moderate agitation at 4 ℃, the plate was centrifuged to collect the elution containing purified IgG. This step was repeated for three times. The purity of eluted IgG was validated by SDS-PAGE and quantified by bicinchoninic acid (BCA) method at 562 nm [20]. The IgG was stored at −80 °C until further use.

2.4. Releasing and labeling of IgG N-glycans

IgG N-glycans were released using the method as reported [29]. Briefly, the purified IgG samples were dissolved in 25 mM ammonium bicarbonate (ABC) at a concentration of 1 mg/ml, and denatured by incubation at 100 °C water bath for 5 min. After cooling to room temperature, 1 μl N-glycosidase F (PNGase F, 500 U/μL) solution was added to release N-glycans overnight at 37 °C. The enzymatic reaction was quenched by a 10 min water bath at 100 °C. The mixtures were immediately put through cotton tips purification or kept in −80 °C for further use [35]. The released N-glycans were then labeled for 2 h at 65 °C with addition of 50 μl 50 mg/ml 2-aminobenzamide (2-AB) and 60 mg/ml

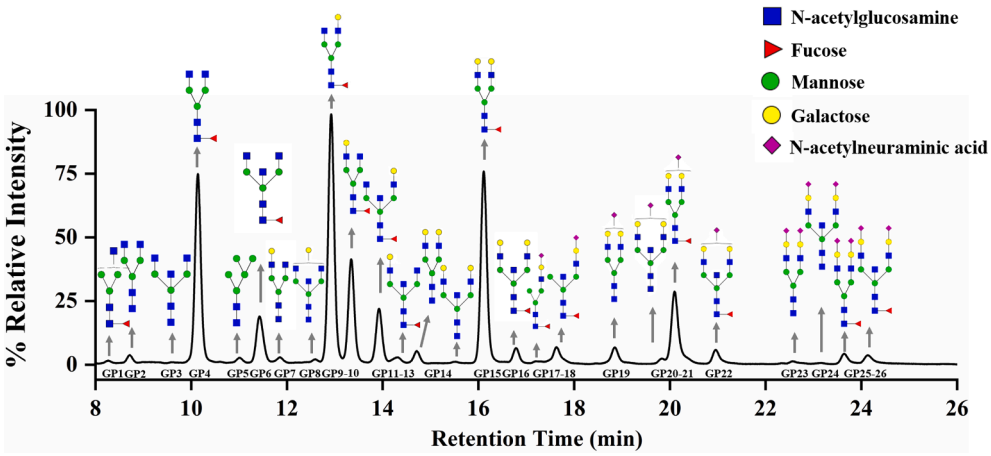

Fig. 1. UPLC analysis of immunoglobulin (IgG) glycosylation. UPLC analysis reveals composition of the glycome which contains 26 chromatographic glycan peaks (GP1–GP26).

$NaBH_3CN$ reductant in a 7:3 (v/v) mixture of DMSO and glacial acetic acid. The labeling reaction was stopped by adding 50 µl water per sample, and then free labeling compound and reductant were removed using cotton tips [35].

2.5. Hydrophilic interaction liquid chromatography (HILIC)-UPLC

Fluorescently labeled N-glycans were separated by HILIC on a Waters ACQUITY(TM) UPLC instrument (Milford, MA, USA) with fluorescence detector set with excitation and emission wavelengths of 330 and 420 nm, respectively. The instrument was operated under the Empower 3 (TM) software (Waters, Milford, MA, USA). The separation of 2-AB labeled N-glycans was performed using ACQUITY(TM) UPLC Glycan BEH(TM) Amide column, 130 Å, 1.7 µm, 2.1 × 150 mm. Mobile phase A and B was water with 100 mM ammonium formate, pH 4.4 and acetonitrile, respectively. Separation method used linear gradient of 75–62% acetonitrile (v/v) at flow rate of 0.4 mL/min in a 30 min analytical run [30]. Samples were maintained at 4 °C before injection, and the separation temperature was 60 °C.

To assign the IgG glycans, one sample was confirmed formerly by comparison with standards (2AB labeled IgG glycan) and also with mass spectrometric profiles of IgG glycans. The separated glycans were analyzed by a Q Exactive mass spectrometry (Thermo Fisher Scientific, Sunnyvale, CA, USA). Mass spectrometry was set as following: positive ion mode, spray voltage, 2.3 kV; the capillary temperature, 320 °C; full MS resolutions, 50,000 at m/z 200. Spectra were first acquired from 100 to 2000 (m/z).

2.6. Data processing and statistical analysis

The chromatographic glycan peaks resulting from the UPLC-fluorescence analysis were processed with Empower 3 software (Waters) using an automated method with a traditional integration algorithm after which each chromatogram was manually corrected to maintain the same intervals of integration for all the samples. The peak signal-to-noise (S/N) ratio detected was above 10. The chromatograms were all separated in the same manner into 26 peaks and the amount of glycans in each peak was expressed as a percentage of the total integrated area. On the basis of these 26 glycans, 64 derived traits were calculated, including the percentage of galactosylation, fucosylation, bisecting GlcNAc, sialylation, and etc. Missing values were imputed with the Bagging Tree algorithm for all data. When imputing missing data, the remaining variables were used as predictors to train the bagging tree, and then to predict missing values. Theoretically, this method is powerful and has a much larger computational load than KNN, and it has higher accuracy [36]. The normalization of data was the entire data divided by the standard deviation. Statistical criteria of Mann-Whitney U test $p < 0.05$ and VIP > 1 was used to evaluate the group difference. The recursive feature elimination (RFE) algorithm was used to screen different numbers of factors. Then logistic regression (LR), and random forest (RF) were used to build the prediction model, which were performed using the sklearn package in Jupyter Notebook 5.7.9. Receiver-operator-characteristics (ROC) test was used to assess the discriminant ability of the glycan traits, and the significance of the resulting values of area-under-the-curve (AUC) was assigned.

3. Results and discussion

3.1. Clinical aspects of the participants

The descriptive information of 98 patients with CE, 29 patients with AE and 22 healthy controls were presented in Table S1, of them 46, 14 and 12 were male, respectively. Mean age of CE, AE patients and healthy controls were 57, 44 and 52 years, respectively, and the cyst sizes were from 1.7*1.7 to 16.2*10.1*8.3. All patients were US diagnosed and serologically confirmed with CE, and the cysts were found at different stages (type CE1, n = 20; type CE2, n = 7; type CE3, n = 33; type CE4, n = 26 and type CE5, n = 12).

3.2. IgG glycan measurement

In this work, N-glycans were released from IgG samples with PNGase F, labeled with 2-AB, purified with cotton tips and analyzed with HILIC-UPLC. Peak assignments were confirmed with standards and determined according to the mass spectrometric profiles of IgG glycans and "GlycoStore" database [30,37]. The fluorescent labeled IgG glycans showed almost identical profiles using fluorescence (FLR) detection which contains 26 chromatographic glycan peaks (GP1–GP26) as shown in Fig. 1. The IgG N-glycan profile was found almost identical in all 149 samples, as shown in Figure S1. At last, 25 IgG glycan chromatographic peaks, and 64 derived traits featuring the glycans derived from galactosylation, fucosylation, bisecting GlcNAc, and sialylation were summarized in Table S2 showing the IgG glycan profile in differentiation of CE, AE and control.

3.3. Serum IgG N-glycome in patients

We discovered that echinococcus infection may change the IgG glycan profiles after additional analysis of the differential expression of IgG N-glycans in patients with CE and AE in comparison to controls. To evaluate the difference between groups analysis of variance (ANOVA) p value was used. We found that 5 IgG N-glycans and 18 glycan derived

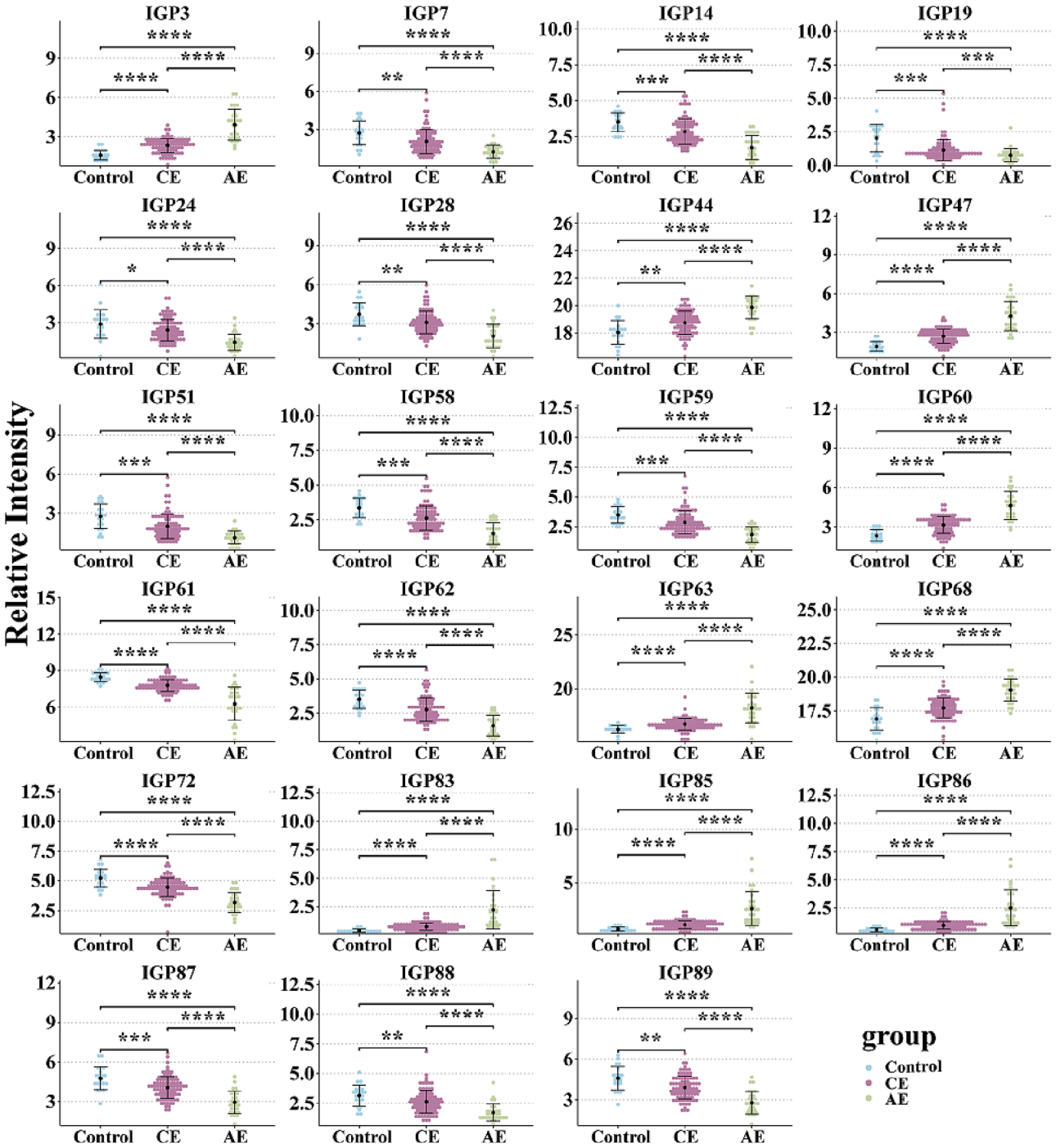

Fig. 2. Scatter plot of altered IgG glycan profiles in CE, AE compared to controls. * indicates p-value < 0.05, ** indicates p-value < 0.01, *** indicates p-value < 0.001 and **** indicates p-value < 0.0001.

traits were different between CE, AE and controls (Table S3). Fig. 2 outlines the changing patterns of 23 IGPs (VIP > 1, p < 0.05). Among them, IGP3 (FA2) was increased, while IGP7 (A2BG1), IGP14 (FA2G2), IGP19 (A2BG2S1) and IGP24 (FA2G2S2) decreased in CE and AE groups. The profiling demonstrated that the neutral glycans, fucosylation and agalactosylated N-glycans increased while sialylation and galactosylation decreased in CE and AE response groups (Table S3). Meanwhile, total neutral glycans (IGP44), fucosylated and agalactosylated N-glycosylation increased while sialylation and galactosylation decreased in response groups (Table S3). Specifically, an increase in agalactosylated glycans FA2 (IGP3 and IGP47) and derived trait IGP60 (G0n), which combines all agalactosylated structures, and a decrease in mono- and di-galactosylated structures (IGP7 and IGP51, A2BG1; IGP14 and IGP58, FA2G2; IGP59, FA2BG2; IGP61, G1n; IGP62, G2n) were associated with CE and AE. The IgG Gal-ratio of IGP83, IGP85, and IGP86 was assayed, which were calculated basedon three ratios G0/[G1 + 2G2], G0n/[G1n + 2G2n] and FG0n/[FG1n + 2FG2n]) [29,38], referring the level of IgG galactosylation. The Gal-ratio was found significantly elevated in CE and AE group (p < 0.0001) (Fig. 2). Higher IgG-galactosylation ratio linked with inflammation was also seen in patients with ankylosing spondylitis and chronic pathology [39,40]. As for sialylation, the mono- and di-sialylated glycan (IGP19, A2BG2S1 and IGP24, FA2G2S2), total sialylated glycans (IGP87, IGP88, IGP89, calculated based on the total mono- and di-sialylated glycan and total

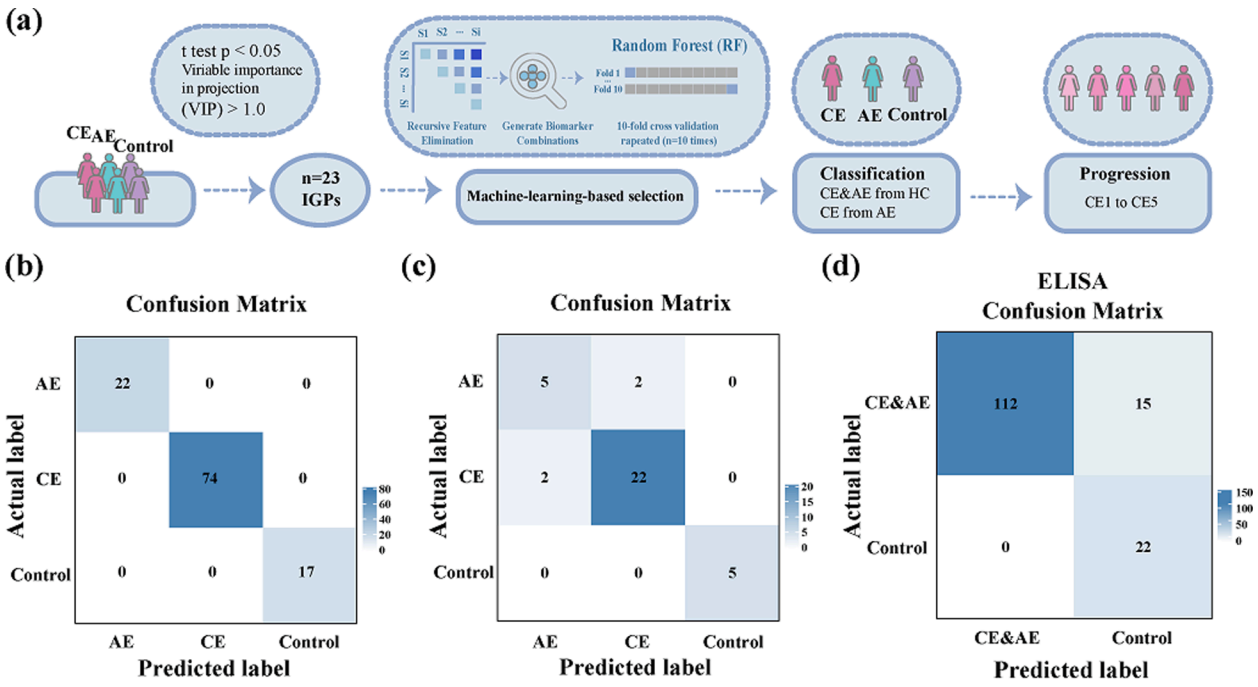

Fig. 3. Machine learning strategy for the classification of CE, AE cases and controls in RF. (a). Workflow of data processing and machine-learning model construction. (b)(c). Confusion matrix of RF model for classifying CE, AE and Control in training cohort (b) and testing cohort (c). (d). Confusion matrix of ELISA.

sialylated glycans) and the percentage of sialylated structures without bisecting GlcNAc (IGP28, calculated by the ratio FGS/[F + FG + FGS]) decreased in patients. The level of bisecting GlcNAc in agalactosylated IgG glycans (IGP72, calculated by FBG0n/G0n) was significantly decreased in CE and AE group ($p < 0.0001$), as well as the fucosylation in agalactosylated glycans (IGP68, calculated by FG0n/G0n) and total fucosylation (IGP63, calculated based on F total) were found to be inversely associated with CE and AE ($p < 0.0001$). These data are in line with those obtained in a *Schistosoma mansoni* infection model, where apoC-III lack sialylation and display a high degree of fucosylation [41]. Our results indicated that *Echinococcus* infection may alter IgG glycosylation, and inferred possible association of galactosylation, sialylation and fucosylation with immune tolerance to the parasite [39].

In order to accurately predict the efficacy of differentiating IgG N-glycans in CE and AE, the machine-learning-based selection of biomarker combinations for classification of CE, AE cases and controls was performed. Model training was carried out based on the glycoforms selected (Fig. 3a), firstly, 23 IGPs were identified as highly ranked differentially expressed glycans (p-value < 0.05 and VIP > 1.0). The recursive feature elimination (RFE) algorithm with cross-validation (10-fold CV, repeated 10 times) was performed to select the optimal biomarker combination on the training set (75% of cohort I), and the accuracy is highest when there are 22 variables in patients compared to controls (Fig. S2a). The variables are shown in Fig. 2 except for the percentage of sialylated structures without bisecting GlcNAc (IGP28, calculated from the ratio FGS/[F + FG + FGS]), and the top 5 variables are IGP63 (total fucosylation, F total), IGP19 (A2BG2S1), GP47 (GP4n), IGP72 (FBG0n/G0n) and IGP61 (G1n) (Fig. S2b). For selection of biomarker combinations, a classification model based on Random forest (RF) algorithm was firstly used. The RF is a machine learning technique to measure the significant degree of predictive parameters, and can produce precise outcomes without over-fitting problem, solving regression problem, classification, and unsupervised learning [42,43]. The optimized RF parameters are obtained by calculating the out-of-bag errors, and the error rate of each classification tends to be flat, indicating that the classification model is robust, and then the RF model is used to train and predict the IgG N-glycans model (Fig. S2c). The learning curve showed the fitting situation of RF classification model based on the accuracy of the training set and the testing set (Fig. S2d). Confusion matrix showing the RF model performance for classifying CE, AE and controls (Fig. 3b), the accuracy was 100% to classify CE, AE and control in the training cohort. Meanwhile, 4 samples were misclassified among testing cohort, and accuracy was 88.9% in classify CE, AE and control (Fig. 3c). However, the combination of UPLC-FLR and machine-learning method is now also providing higher specificity, compared with anti-*Echinococcus* IgG antibody ELISA. While immunoassay methods have dominated clinical analyses, ELISA can just distinguish echinococcosis compared to controls, and it is unable to distinguish AE from and CE. When determining whether having echinococcosis, the specificity of RF model has very little difference compared with the result of ELISA (Table S4), thus adding glycans to the clinical variables may improve the prediction. Confusion matrix demonstrated that better accuracy was observed using RF prediction model with IgG glycan variables than by ELISA. In the model computation, 15 samples (accuracy: 89.9%) were misclassified between echinococcosis and controls (Fig. 3d) while no samples (accuracy: 100%) were misclassified among training cohort and 4 samples (accuracy: 88.9%) were misclassified among testing cohort (Fig. 3b-c).

We also used clustering method to further assess these IGPs. Clustering methods can reveal hidden-patterns in large complex data sets. Mfuzz is a clustering method software, and can assign IGPs to several clusters if their expression patterns are similar [44]. The expression trends of IGPs were divided into 6 categories by Mfuzz, in which the yellow and green lines indicated the IGPs with small differences in expression in different groups, and the red and purple lines indicated the IGPs with large differences in these three groups (Figure S3). Then, 22 IGP factors were extracted from the Mfuzz clustering and made into a line trend graph. As shown in Figure S4, a remarkable feature of echinococcosis is the upregulation of cluster 3 and 5 in patients compared to controls, whereas the downregulation of cluster 1, 2 and 6 in CE and AE. We found the IGPs in the cluster 3 were mainly the ratio of galactosylated structures in total neutral IgG glycans and most fucosylated and netural glycans were clustered into cluster 5, while the most sialylated N-glycans were clustered into cluster 2 and 6. It is suggested that the downregulation of sialylation occurred in CE and AE, and there is a possibility that different types of N-glycans may play different roles in

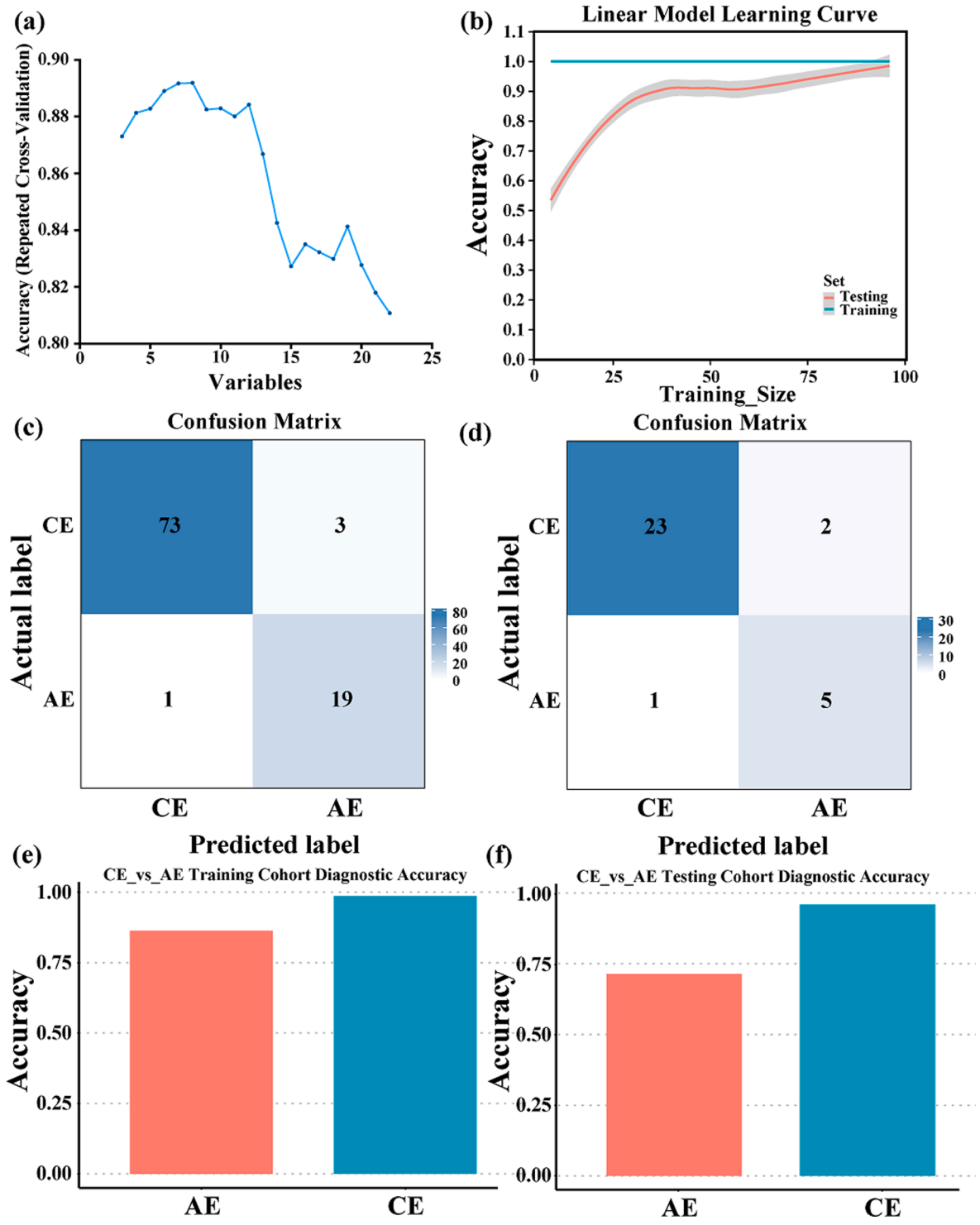

Fig. 4. Machine learning strategy for the classification of CE and AE cases in LR. (a). The accuracy of different number of variables. (b). The learning curve showing the fitting situation of RF model based on the accuracy of the training set and the testing set. (c)(d). Confusion matrix of LR model for classifying CE and AE in training cohort (c) and testing cohort (d). (e)(f).The accuracy of training (e) and testing cohort (f).

these three groups, which indicated that N-glycans synthesis may change in human body during the development of echinococcosis.

To better differentiate CE and AE, logistic regression (LR) was also conducted. Logistic regression is a classical and prominent method for classification and it is used as benchmark for comparing the alternative methods [45]. The accuracy is highest when there are 8 variables (IGP59, IGP63, IGP68, IGP83, IGP86, IGP87, IGP88 and IGP89) in patients with AE compared to CE (Fig. 4a). Among the 8 IGPs, the IGP63, IGP83, IGP86 were included in the sets of biomarkers to distinguish CE from controls; all these 8 IGPs were included in the biomarker sets, which could accurately distinguish AE from controls. The learning curve showed good fitting of LR model based on the accuracy of the training set and the testing set (Fig. 4b). Confusion matrix indicated that with the LR model (Fig. 4c-d), the accuracy to classify CE and AE was 93% in the training cohort and 3 samples were misclassified among testing cohort (Fig. 4d), showing better accuracy than using RF model (Fig. 3c). With a

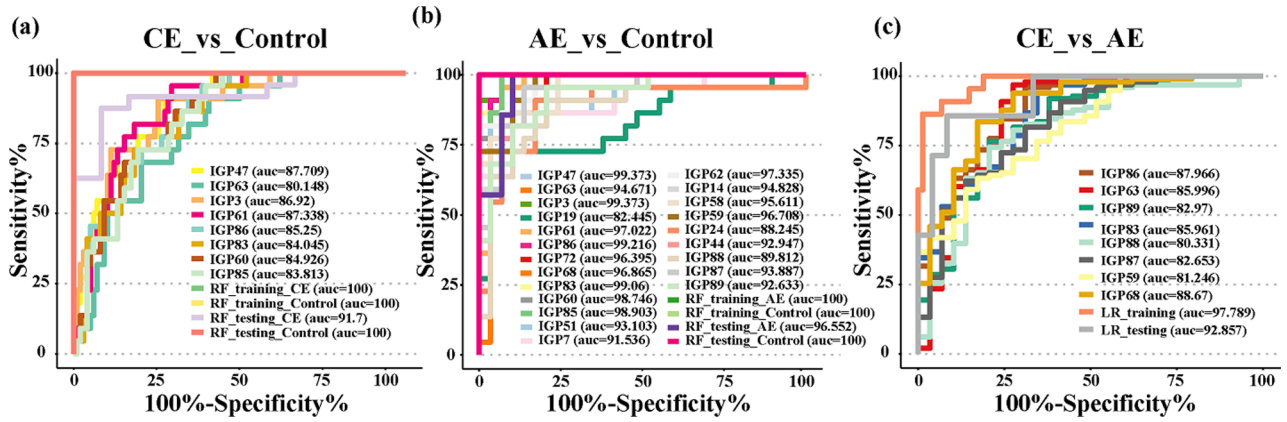

Fig. 5. Receiver operating characteristic (ROC) curve analyses for the N-glycans with AUC above 0.8 of CE vs Control (a), AE vs Control (b) and CE vs AE (c).

better classification performance, the LR model is recommended for future applications in classification of CE and AE.

We further performed the receiver operating characteristic (ROC) curve analysis for serum IgG N-glycans, and found three biomarker combinations could differentiate AE,CE and controls. The area-under-the-curve (AUC) evaluates the performance of a classifier, and a higher AUC means a better classification. The AUC value above 0.8 is considered as acceptable to excellent accuracy [46,47]. Through the N-glycan abundance analysis and machine-learning-based selection of biomarker combinations, we found that 8 IGPs have significant differences in the serum IgG of patients with CE (Fig. 5a), while 22 IGPs have significant differences in AE patients, compared with controls (Fig. 5b). The accuracy is highest when there are 8 variables in CE patients, and in the training set of CE in RF model, the AUC of ROC was 1, while in the testing set of CE, the AUC was 0.917 (95% CI = 0.825–1). Similar to the analysis of CE compared to controls, the accuracy is highest when there are 22 variables in patients with AE compared to controls, and in the training set of AE in RF, the AUC of ROC was 1, while the AUC of ROC was 0.966 (95% CI = 0.912–1) in the testing set of AE. In the differentiation of CE and AE, the ROC of LR was further constructed. Similarly, the accuracy is highest when there are 8 variables to differentiate CE and AE, and the AUC of ROC was 0.978 (95% CI = 0.953–1) in the training set, while the AUC of ROC was 0.929 (95% CI = 0.827–1) in the testing set (Fig. 5c). Other diagnostic performance was shown in Table S5. Therefore, the potential biomarkers combinations could accurately distinguish CE and AE from controls.

To our knowledge, this is the first study to investigate the potential role of IgG glycome in echinococcosis. Alteration of IgG glycome correlates with some inflammatory diseases and infectious diseases including parasitic infections, such as leishmaniasis and filariasis [48–50]. Therefore, study of glycome profiles of IgG could not only yield new diagnostic markers, but is also key to understanding pathogenicity, and could give rise to new principles for preventing and treating infectious diseases [48]. According to the statistical result, the galactosylation, sialylation and fucosylation are closely related to echinococcosis and these changes could distinguish between CE, AE and controls. Some studies have suggested possible mechanism for the change of IgG galactosylation ratio in autoimmune diseases and cancers, such as downregulated galactosyltransferase activity in plasma cells [51] or host-defense response to the presence of the tumor [52]. Also, the alteration of sialylated N-glycans was associated with the promotion of invasion and metastasis of CRC and other cancers [29], and higher IgG-galactosylation linked with inflammation was also seen in patients with ankylosing spondylitis and chronic pathology [39,40], inferring that N-glycan profile could be potential biomarker for CE and AE. Abnormal total fucosylation (IGP63, F total) was found elevated in CE and AE, and the elevation was more evident in AE, indicating the fucosylation contributes to AE progression. Our data suggest that fucosylation was high in CE and AE than controls. The high level of IgG fucosylation was also observed in filarial infections [39]. Though little is known on IgG fucosylation in echinococcosis, studies demonstrated fucosylation of glycoproteins was observed in several cancers, such as prostate cancer [53], endometrial cancer [54] and pancreatic cancer [55], playing a role in proliferation, invasion, metastasis, and immune escape. Fucosylation of protein is regulated by Fut8 and fucosidase, and the decrease of fucosylation may be caused by the down-regulation of Fut8 expression [56] and/or up-regulation of fucosidas expression [57]. Early diagnosis of CE and AE can provide significant improvements in the quality of the management and treatment. Particularly, early detection of AE is more paramount because of its higher mortality. As shown in Fig. 5, we identified 22 IgG glycan traits with high statistical significance associated with AE and 8 IgG glycan traits with high statistical significance associated with CE, it seems that AE is more significant than CE in diagnosis, and our findings were in line with previous study that serological tests for antibody detection are generally more reliable [58]. Our findings suggest a new approach to deeper understand the role of IgG glycosylation in echinococcosis. However, the enzymatic mechanism of glycosylation under pathologic status remains to be further elucidated.

3.4. Serum IgG N-glycome in patients with different types of CE

The differentiated cyst types were classified into three groups: active (CE1 and CE2), transitional (CE3) and inactive (CE4 and CE5) [17]. To explore the early diagnostic biomarkers of CE, we subsequently investigated the potential response of serum IgG N-glycans in differentiation of the CE types, and evidenced that IGP88 (di-sialylated glycan) could distinguish CE3&4 from CE5. The heatmap of hierarchical clustering (Figure S5) showed that there is a clear difference between controls and CE as mentioned above, and also indicated the IGPs altered in different groups from CE1 to CE5. Mfuzz clustering analysis presented that the expression trends of IGPs were divided into 3 categories, from which 22 IGP factors were extracted to plot a line trend graph. As shown in Fig. 6a, the “Gal-ratio” (IGP83, IGP85, IGP86, calculated by three ratios G0/[G1 + 2G2],G0n/[G1n + 2G2n] and FG0n/[FG1n + 2FG2n]) in cluster 3 were significantly elevated in patients with cyst type CE1 (early stage) compared to controls, whereas the level of these three IGPs markedly declined at stage CE4 and CE5. However, the other six IGPs in cluster 3 showed slight increase upon the CE1 stage and slight decrease from CE3 stage to CE5 stage. Conversely, the downregulation of CE1 in cluster 2 was observed, whereas the level of these IGPs in cluster 2 increased at stage CE2. It is suggested that the downregulation of sialylation occurred in CE progression, indicating that N-glycans synthesis may change in human body during the development of CE. We further evaluated the differentially expressed IgG N-glycome in patients with CE1-5. Fig. 6b outlines the changing patterns of IGP19 and IGP59, which can better

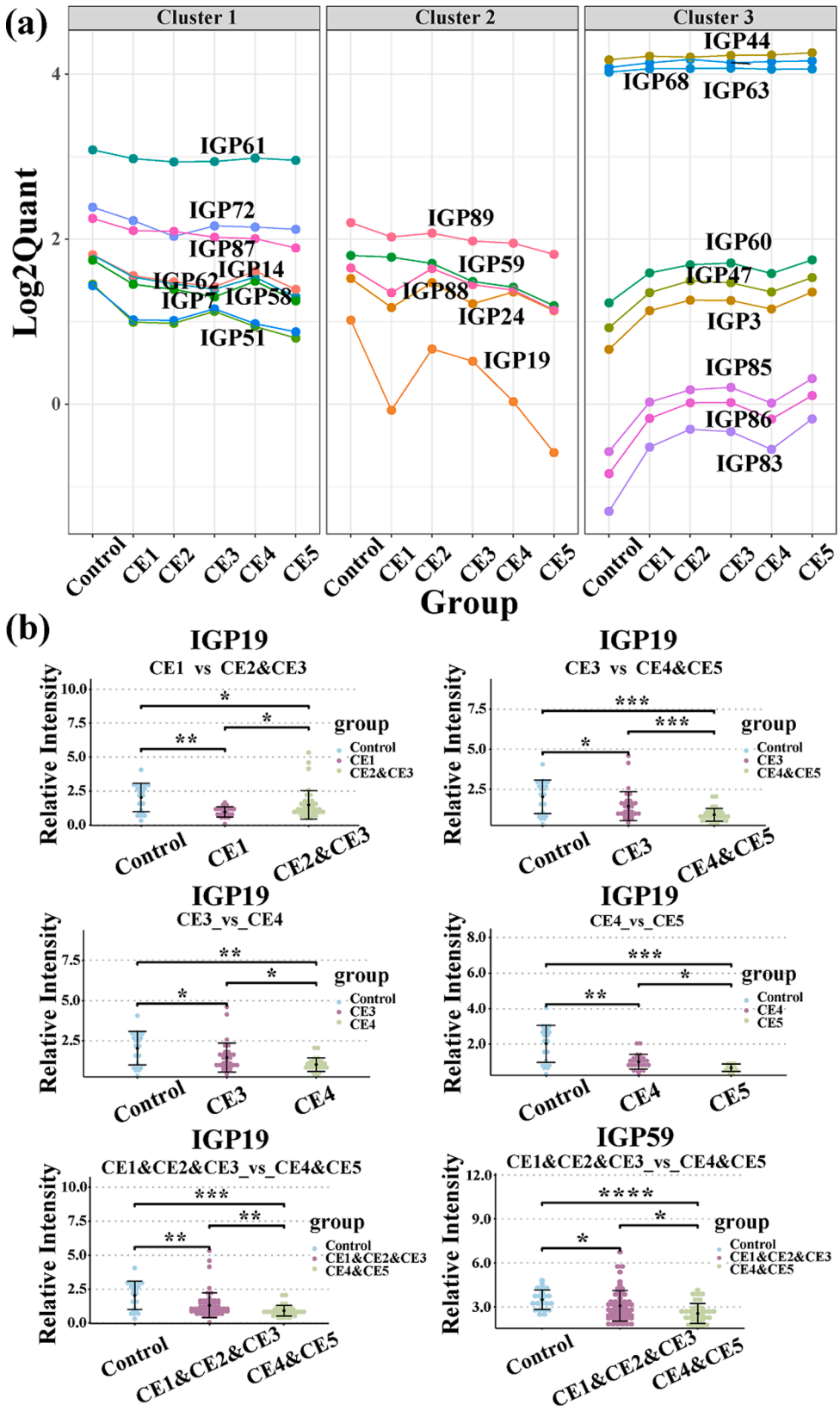

Fig. 6. Changes of IgG glycan profiles according to CE progression. (a). Clusters of altered IgG glycan profiles in CE1-CE5. (b). Scatter plot of altered IgG glycan profiles in CE1-5 compared to controls. * indicates p-value < 0.05, ** indicates p-value < 0.01, *** indicates p-value < 0.001 and **** indicates p-value < 0.0001.

distinguish CE1-5 between these two states. We noted that the level of IGP19 (A2BG2S1) was significantly altered in different types of CE. It showed that the sialylated structures in total IgG glycans were decreased in CE different stages in patients. IGP19 (A2BG2S1) not only can distinguish the CE patients from controls, but also can distinguish CE1 and CE2&3, CE3 and CE4&5, CE3 and CE4, CE4 and CE5 and CE1&2&3 and CE4&5. IGP59 (FA2BG2) can also be used to distinguish CE1&2&3 and CE4&5. The ROC curves are shown in Figure S6. It also showed that IGP88 (di-sialylated glycan) can be used to distinguish CE3&4 from CE5. Cystic echinococcosis is a chronic and complex zoonosis, the proposed method showed that glycan profiles is associated with cyst development.

3.5. IgG N-glycan dynamic profile in follow-up patients

To explore the potential tracking and monitoring value of IgG N-glycans in CE, we further assessed the dynamic changes of IGP19 levels in five follow-up CE patients over three years. Each patient (P1-P5) presented a disease progress path (either P1/CE1-CE4-CE4, P2/CE1-CE4-CE4, P3/CE3-CE3-CE4, P4/CE4-CE4-CE3 or P5/CE3-CE3-CE4 on yearly basis) during the three-year period, exhibiting corresponding IgG glycomic responses as shown in Figure S7. To examine the cyst stage-related IgG glycomics, we analyzed the level of IGP19 of individual patients by plotting the cyst stage (CE1-CE5) against the relative intensity of IGP19 to show a dynamic change. We found that P1 and P2 underwent changes from stage CE1 in Year 1 to CE4 in Year 2 and Year 3, while the IGP19 level exhibited a increasing trend from CE1 to CE4 and then declined in Year 3 which may be indicated that the further development of the disease. The result suggests that IGP19 could be a potential biomarker for early diagnosis. The IGP19 of patient 3 (P3) and patient 5 (P5) were highly expressed at type CE3, whereas their levels markedly declined at stage CE4. In patient 4 (P4), IGP19 was also lowly expressed at stage CE4 while their levels markedly increased at stages CE3. For further study, an appropriate follow-up sample size is essential for gaining insight into the interplay between IgG glycome and antibodies, and additional investigations with larger cohorts are required to define the relationship between glycosylation and CE progression. The US pathognomonic image and confirmatory serological test may benefit from the IgG glycan typing of CE1-5 for early diagnosis. Additionally, the N-glycan profiling method may be used to assess CE disease development and distinguish between disease stages.

4. Conclusion

In summary, this is the first study on serum IgG glycome profiling in patients with CE, AE compared with controls. The neutral glycans, fucosylation and agalactosylated N-glycans increased while sialylation and galactosylation decreased in echinococcosis patients. Combined with a machine-learning-based technique, we demonstrated potential biomarker combinations of IgG N-glycans could distinguish CE, AE from controls with high accuracy. Our results also demonstrated that IgG glycans of CE patients were altered along with the disease progression and they differed from one another. The profile change suggests that the glycosylation and immune response may play a role in the progression of cyst degeneration. However, to date, there are no intensive studies of immunological events associated with the degeneration of different types of cyst. Furthermore, the biological mechanism for such a relationship has yet to be determined. For future study, better understanding of the role of IgG glycosylation may lead to a new way to meet the challenge in stage-differentiation and early diagnosis of echinococcosis.

5. Ethics approval and consent to participate

The acquisition and use of this experimental specimen was approved by the Ethics Committee of the National Institute of Parasitic Diseases, Chinese Center for Disease Control and Prevention (NIPD/China CDC, Approval Number: 20130516). All procedures including blood sample collection and clinical examinations complied with the guideline of the Committee and were conducted in accordance with the approved research protocol. The study purpose and procedures were explained to the donors and/or guardians, and their written informed consent was obtained. All personal data were kept confidential.

CRediT authorship contribution statement

Xiaoxiao Feng: Methodology, Data curation, Writing - original draft. **BaiMaYangJin:** Methodology, Writing - review & editing. **Xiaojin Mo:** Methodology, Writing - review & editing. **Fangyan Zhang:** Methodology, Writing - review & editing. **Wei Hu:** Methodolog, Writing - review & editing. **Zheng Feng:** Writing - review & editing. **Ting Zhang:** Methodology, Writing - review & editing, Resources. **Liming Wei:** Project adminstration, Funding acquisition, Writing - review & editing. **Haojie Lu:** Project adminstration, Funding acquisition, Writing - review & editing, Supervision, Resources.

Declaration of Competing Interest

The authors declare that they have no known competing financial interests or personal relationships that could have appeared to influence the work reported in this paper.

Data availability

Data will be made available on request.

Acknowledgment

The work was supported by the Shanghai Science and Technology Program (22DZ2291700 and 22142202400), the National Key Research and Development Program of China (2016YFA0501303 and 2020YFE0202200), the NHC Key Laboratory of Echinococcosis Prevention and Control (Project No. 2020WZK2006), NSF of China (Grants 21974025), Shanghai Pujiang Program (18PJD002), and the Non-profit Central Research Institute Fund of Chinese Academy of Medical Sciences (No. 2019PT320004).

Appendix A. Supplementary data

Supplementary data to this article can be found online at https://doi.org/10.1016/j.jchromb.2023.123838.

References

[1] P. Kern, A.M. da Silva, O. Akhan, B. Mullhaupt, K.A. Vizcaychipi, C. Budke, D. A. Vuitton, The Echinococcoses: Diagnosis, Clinical Management and Burden of Disease, in: R.C.A. Thompson, P. Deplazes, A.J. Lymbery (Eds.), Echinococcus and Echinococcosis, Elsevier Academic Press Inc, San Diego, Pt B, 2017, pp. 259–369.
[2] D.P. McManus, D.J. Gray, W.B. Zhang, Y.R. Yang, Diagnosis, treatment, and management of echinococcosis, Bmj-British Medical Journal 344 (2012) e3866.
[3] C.M. Budke, H. Carabin, P.C. Ndimubanzi, N. Hai, E. Rainwater, M. Dickey, R. Bhattarai, O. Zeziulin, M.-B. Qian, A Systematic Review of the Literature on Cystic Echinococcosis Frequency Worldwide and Its Associated Clinical Manifestations, Am. J. Trop. Med. Hyg. 88 (2013) 1011–1027.
[4] P.R. Torgerson, K. Keller, M. Magnotta, N. Ragland, The Global Burden of Alveolar Echinococcosis, PLoS Negl. Trop. Dis. 4 (2010) e722.
[5] L.Y. Wang, M. Qin, Z.H. Liu, W.P. Wu, N. Xiao, X.N. Zhou, S. Manguin, L. Gavotte, R. Frutos, Prevalence and spatial distribution characteristics of human echinococcosis in China, PLoS Negl. Trop. Dis. 15 (2021) e0009996.
[6] H. Ghasemirad, N. Bazargan, A. Shahesmaeili, M.F. Harandi, Echinococcosis in immunocompromised patients: A systematic review, Acta Trop. 232 (2022), 106490.
[7] https://www.who.int/news-room/fact-sheets/detail/echinococcosis.
[8] P.S. Craig, E. Larrieu, Control of cystic echinococcosis/hydatidosis: 1863–2002, in: D.H. Molyneux (Ed.), Advances in Parasitology, Vol 61: Control of Human Parasitic Diseases, Elsevier Academic Press Inc, San Diego, 2006, pp. 443–487.
[9] F. Lotsch, C.M. Budke, H. Auer, K. Kaczirek, F. Waneck, H. Lagler, M. Ramharter, Evaluation of direct costs associated with alveolar and cystic echinococcosis in Austria, PLoS Negl. Trop. Dis. 13 (2019) e0007110.

[10] P.R. Torgerson, L.J. Robertson, H.L. Enemarkx, J. Foehr, J.W.B. van der Giessen, C. M.O. Kapel, I. Klun, C. Trevisan, Source attribution of human echinococcosis: A systematic review and meta-analysis, PLoS Negl. Trop. Dis. 14 (2020) e0008382.

[11] M. Borhani, S. Fathi, S. Lahmar, H. Ahmed, M.F. Abdulhameed, M.F. Harandi, Cystic echinococcosis in the Eastern Mediterranean region: Neglected and prevailing!, PLoS Negl. Trop. Dis. 14 (2020) e0008114.

[12] H. Wen, L. Vuitton, T. Tuxun, J. Li, D.A. Vuitton, W.B. Zhang, D.P. McManus, Echinococcosis: Advances in the 21st Century, Clin. Microbiol. Rev. 32 (2019) e00075–e00118.

[13] P.R. Torgerson, B. Devleesschauwer, N. Praet, N. Speybroeck, A.L. Willingham, F. Kasuga, M.B. Rokni, X.N. Zhou, E.M. Fevre, B. Sripa, N. Gargouri, T. Furst, C. M. Budke, H. Carabin, M.D. Kirk, F.J. Angulo, A. Havelaar, N. de Silva, World Health Organization Estimates of the Global and Regional Disease Burden of 11 Foodborne Parasitic Diseases, 2010: A Data Synthesis, PLoS Med. 12 (2015) e1001920.

[14] S. Baumann, R. Shi, W.Y. Liu, H.H. Bao, J. Schmidberger, W. Kratzer, W.X. Li, T.F. E. Barth, S. Baumann, J. Bloehdorn, I. Fischer, T. Graeter, N. Graf, B. Gruener, D. Henne-Bruns, A. Hillenbrand, T. Kaltenbach, P. Kern, P. Kern, K. Klein, W. Kratzer, N. Ehteshami, P. Schlingeloff, J. Schmidberger, R. Shi, Y. Staehelin, F. Theis, D. Verbitskiy, G. Zarour, E. Interdisciplinary, Worldwide literature on epidemiology of human alveolar echinococcosis: a systematic review of research published in the twenty-first century, Infection 47 (2019) 703–727.

[15] A. Khan, H. Ahmed, H. Khan, S. Saleem, S. Simsek, E. Brunetti, M.S. Afzal, T. Manciulli, C.M. Budke, Cystic Echinococcosis in Pakistan: A Review of Reported Cases, Diagnosis, and Management, Acta Tropica 212 (2020), 105709.

[16] W. Hosch, T. Junghanss, M. Stojkovic, E. Brunetti, T. Heye, G.W. Kauffmann, W. E. Hull, Metabolic viability assessment of cystic echinococcosis using high-field H-1 MRS of cyst contents, NMR Biomed. 21 (2008) 734–754.

[17] Z.D. Li, X.J. Mo, S. Yan, D. Wang, B. Xu, J. Guo, T. Zhang, W. Hu, Y. Feng, X. N. Zhou, Z. Feng, Multiplex cytokine and antibody profile in cystic echinococcosis patients during a three-year follow-up in reference to the cyst stages, Parasit Vectors 13 (2020) 133.

[18] W. Zhang, H. Wen, J. Li, R. Lin, D.P. McManus, Immunology and immunodiagnosis of cystic echinococcosis: an update, Clin. Dev. Immunol. 2012 (2012), 101895.

[19] M.D. Larsen, E.L. de Graaf, M.E. Sonneveld, H.R. Plomp, J. Nouta, W. Hoepel, Afucosylated IgG characterizes enveloped viral responses and correlates with COVID-19 severity, Science 371 (2021) 907–915.

[20] L.J. Yang, Z.Y. Sun, L. Zhang, Y. Cai, Y. Peng, T. Cao, Y. Zhang, H.J. Lu, Chemical labeling for fine mapping of IgG N-glycosylation by ETD-MS, Chem. Sci. 10 (2019) 9302–9307.

[21] M. Siles-Lucas, A. Casulli, F.J. Conraths, N. Muller, Laboratory Diagnosis of Echinococcus spp. in Human Patients and Infected Animals, in: R.C.A. Thompson, P. Deplazes, A.J. Lymbery (Eds.) Echinococcus and Echinococcosis, Pt B2017, pp. 159-257.

[22] K. Ohtsubo, J.D. Marth, Glycosylation in cellular mechanisms of health and disease, Cell 126 (2006) 855–867.

[23] S. Esmail, M.F. Manolson, Advances in understanding N-glycosylation structure, function, and regulation in health and disease, Eur. J. Cell Biol. 100 (2021), 151186.

[24] P.M. Rudd, T. Elliott, P. Cresswell, I.A. Wilson, R.A. Dwek, Glycosylation and the immune system, Science 291 (2001) 2370–2376.

[25] A. Helenius, M. Aebi, Roles of N-linked glycans in the endoplasmic reticulum, Annu. Rev. Biochem 73 (2004) 1019–1049.

[26] S.S. Pinho, C.A. Reis, Glycosylation in cancer: mechanisms and clinical implications, Nat. Rev. Cancer 15 (2015) 540–555.

[27] M. Simurina, N. de Haan, F. Vuckovic, N.A. Kennedy, J. Stambuk, D. Falck, I. Trbojevic-Akmacic, F. Clerc, G. Razdorov, A. Khon, A. Latiano, R. D'Inca, S. Danese, S. Targan, C. Landers, M. Dubinsky, D.P.B. McGovern, V. Annese, M. Wuhrer, G. Lauc, B. Inflammatory Bowel Dis, Glycosylation of Immunoglobulin G Associates With Clinical Features of Inflammatory Bowel Diseases, Gastroenterology, 154 (2018) 1320-1333.

[28] L. Klaric, Y.A. Tsepilov, C.M. Stanton, M. Mangino, T.T. Sikka, T. Esko, E. Pakhomov, P. Salo, J. Deelen, S.J. McGurnaghan, T. Keser, F. Vuckovic, I. Ugrina, J. Kristic, I. Gudelj, J. Stambuk, R. Plomp, M. Pucic-Bakovic, T. Pavic, M. Vilaj, I. Trbojevic-Akmacic, C. Drake, P. Dobrinic, J. Mlinarec, B. Jelusic, A. Richmond, M. Timofeeva, A.K. Grishchenko, J. Dmitrieva, M.L. Bermingham, S. Z. Sharapov, S.M. Farrington, E. Theodoratou, H.W. Uh, M. Beekman, E. P. Slagboom, E. Louis, M. Georges, M. Wuhrer, H.M. Colhoun, M.G. Dunlop, M. Perola, K. Fischer, O. Polasek, H. Campbell, I. Rudan, J.F. Wilson, V. Zoldos, V. Vitart, T. Spector, Y.S. Aulchenko, G. Lauc, C. Hayward, Glycosylation of immunoglobulin G is regulated by a large network of genes pleiotropic with inflammatory diseases, Science, Advances 6 (2020) eaax0301.

[29] S.F. Ren, Z.J. Zhang, C.J. Xu, L. Guo, R.Q. Lu, Y.H. Sun, J.M. Guo, R.H. Qin, W. J. Qin, J.X. Gu, Distribution of IgG galactosylation as a promising biomarker for cancer screening in multiple cancer types, Cell Res. 26 (2016) 963–966.

[30] E. Theodoratou, K. Thaci, F. Agakov, M.N. Timofeeva, J. Stambuk, M. Pucic-Bakovic, F. Vuckovic, P. Orchard, A. Agakova, F.V.N. Din, E. Brown, P.M. Rudd, S. M. Farrington, M.G. Dunlop, H. Campbell, G. Lauc, Glycosylation of plasma IgG in colorectal cancer prognosis, Sci Rep 6 (2016) 12.

[31] Z.Y. Wu, H.B. Li, D. Liu, L.X. Tao, J. Zhang, B.L. Liang, X.T. Liu, X.N. Wang, X. Li, Y. X. Wang, W. Wang, X.H. Guo, IgG Glycosylation Profile and the Glycan Score Are Associated with Type 2 Diabetes in Independent Chinese Populations: A Case-Control Study, Journal of Diabetes Research 2020 (2020) 1–8.

[32] A. van Diepen, N.S.J. van der Velden, C.H. Smit, M.H.J. Meevissen, C.H. Hokke, Parasite glycans and antibody-mediated immune responses in Schistosoma infection, Parasitology 139 (2012) 1219–1230.

[33] I.F. Rehan, M.E. Mahmoud, D. Salman, A. Elnagar, S. Salman, M. Youssef, A.R. A. Aziz, E.K. Bazh, A. Hesham, Sialylated N-glycan profile during acute and chronic infections with Toxoplasma gondii in mice, Sci Rep 10 (2020) 3809.

[34] J. Sotillo, A. Cortes, C. Munoz-Antoli, B. Fried, J.G. Esteban, R. Toledo, The effect of glycosylation of antigens on the antibody responses against Echinostoma caproni (Trematoda: Echinostomatidae), Parasitology 141 (2014) 1333–1340.

[35] Y. Peng, J. Lv, L.J. Yang, D.Q. Wang, Y. Zhang, H.J. Lu, A streamlined strategy for rapid and selective analysis of serum N-glycome, Anal. Chim. Acta 1050 (2019) 80–87.

[36] L. Breiman, Bagging predictors, Mach. Learn. 24 (1996) 123–140.

[37] T. Keser, T. Pavic, G. Lauc, O. Gornik, Comparison of 2-Aminobenzamide, Procainamide and RapiFluor-MS as Derivatizing Agents for High-Throughput HILIC-UPLC-FLR-MS N-glycan Analysis, Front. Chem. 6 (2018) 12–23.

[38] A.L. Zhong, R.H. Qin, W.J. Qin, J. Han, Y. Gu, L. Zhou, H.Q. Zhang, S.F. Ren, R. Q. Lu, L. Guo, J.X. Gu, Diagnostic Significance of Serum IgG Galactosylation in CA19-9-Negative Pancreatic Carcinoma Patients, Front. Oncol. 9 (2019) 114.

[39] T. Adjobimey, A. Hoerauf, Distinct N-Linked Immunoglobulin G Glycosylation Patterns Are Associated With Chronic Pathology and Asymptomatic Infections in Human Lymphatic Filariasis, Front. Immunol. 13 (2022), 790895.

[40] J. Liu, Q. Zhu, J. Han, H. Zhang, Y. Li, Y.Y. Ma, H.D. Ji, D.Y. He, J.X. Gu, X.D. Zhou, J.D. Reveille, L. Jin, H.J. Zou, S.F. Ren, J.C. Wang, The IgG galactosylation ratio is higher in spondyloarthritis patients and associated with the MRI score, Clin. Rheumatol. 39 (2020) 2317–2323.

[41] C.I.A. Balog, O.A. Mayboroda, M. Wuhrer, C.H. Hokke, A.M. Deelder, P. J. Hensbergen, Mass Spectrometric Identification of Aberrantly Glycosylated Human Apolipoprotein C-III Peptides in Urine from Schistosoma mansoni-infected Individuals, Mol. Cell. Proteomics 9 (2010) 667–681.

[42] G. Izmirlian, Application of the random forest classification algorithm to a SELDI-TOF proteomics study in the setting of a cancer prevention trial, in: A. Umar, I. Kapetanovic, J. Khan (Eds.) Applications of Bioinformatics in Cancer Detection 2004, pp. 154-174.

[43] L.F. Montano-Gutierrez, S. Ohta, G. Kustatscher, W.C. Earnshaw, J. Rappsilber, Nano Random Forests to mine protein complexes and their relationships in quantitative proteomics data, Mol. Biol. Cell 28 (2017) 673–680.

[44] L. Kumar, M.E. Futschik, Mfuzz: a software package for soft clustering of microarray data, Bioinformation 2 (2007) 5–7.

[45] L. Yan, J. Yi, C.W. Huang, J. Zhang, S.H. Fu, Z.J. Li, Q. Lyu, Y. Xu, K. Wang, H. Yang, Q.W. Ma, X.P. Cui, L. Qiao, W. Sun, P. Liao, Rapid Detection of COVID-19 Using MALDI-TOF-Based Serum Peptidome Profiling, Anal. Chem. 93 (2021) 4782–4787.

[46] X. Robin, N. Turck, A. Hainard, N. Tiberti, F. Lisacek, J.C. Sanchez, M. Muller, pROC: an open-source package for R and S plus to analyze and compare ROC curves, BMC Bioinf. 12 (2011) 77–84.

[47] J.N. Mandrekar, Receiver Operating Characteristic Curve in Diagnostic Test Assessment, J. Thorac. Oncol. 5 (2010) 1315–1316.

[48] S. Onsurathum, M.J. Kailemia, K. Intuyod, O. Haonon, C. Pairojkul, R. Thanan, P. Pinlaor, C.B. Lebrilla, S. Pinlaor, N-glycosylation profiling of serum immunoglobulin in opisthorchiasis patients, J. Proteomics 230 (2021), 103980.

[49] N.L. O'Regan, S. Steinfelder, C. Schwedler, G.B. Rao, A. Srikantam, V. Blanchard, S. Hartmann, Filariasis asymptomatically infected donors have lower levels of disialylated IgG compared to endemic normals, Parasite Immunol. 36 (2014) 713–720.

[50] L.G. Gardinassi, V. Dotz, A.H. Ederveen, R.P. de Almeida, C.H.N. Costa, D.L. Costa, A.R. de Jesus, O.A. Mayboroda, G.R. Garcia, M. Wuhrer, I. Santosa, Clinical Severity of Visceral Leishmaniasis Is Associated with Changes in Immunoglobulin G Fc N-Glycosylation, MBio 5 (2014) e01844.

[51] J.S. Axford, N. Sumar, A. Alavi, D.A. Isenberg, A. Young, K.B. Bodman, I.M. Roitt, Changes in normal glycosylation mechanisms in autoimmune rheumatic disease, J. Clin. Investig. 89 (1992) 1021–1031.

[52] J. Bones, J.C. Byrne, N. O'Donoghue, C. McManus, C. Scaife, H. Boissin, A. Nastase, P.M. Rudd, Glycomic and Glycoproteomic Analysis of Serum from Patients with Stomach Cancer Reveals Potential Markers Arising from Host Defense Response Mechanisms, J. Proteome Res. 10 (2011) 1246–1265.

[53] D.J. Clark, M. Schnaubelt, N. Hoti, Y.W. Hu, Y.Y. Zhou, M. Gooya, H. Zhang, Impact of Increased FUT8 Expression on the Extracellular Vesicle Proteome in Prostate Cancer Cells, J. Proteome Res. 19 (2020) 2195–2205.

[54] H. Shimoyama, T.K. Shibata, M. Ito, T. Oda, T. Itoh, M. Mukai, M. Matsuya-Ogawa, M. Adachi, H. Murakami, T. Nakayama, K. Sugihara, H. Itoh, T. Suzuki, N. Kanayama, Partial silencing of fucosyltransferase 8 gene expression inhibits proliferation of Ishikawa cells, a cell line of endometrial cancer, Biochem. Biophys. Rep. 22 (2020), 100740.

[55] K. Tada, M. Ohta, S. Hidano, K. Watanabe, T. Hirashita, Y. Oshima, A. Fujnaga, H. Nakanuma, T. Masuda, Y. Endo, Y. Takeuchi, Y. Iwashita, T. Kobayashi, M. Inomata, Fucosyltransferase 8 plays a crucial role in the invasion and metastasis of pancreatic ductal adenocarcinoma, Surg. Today 50 (2020) 767–777.

[56] Y.P. Zhao, C.P. Ruan, H. Wang, Z.Q. Hu, M. Fang, X. Gu, J. Ji, J.Y. Zhao, C.F. Gao, Identification and assessment of new biomarkers for colorectal cancer with serum N-glycan profiling, Cancer 118 (2012) 639–650.

[57] S.D. Szajda, J. Snarska, Z. Puchalski, K. Zwierz, Lysosomal exoglycosidases in serum and urine of patients with colon adenocarcinoma, Hepatogastroenterology 55 (2008) 921–925.

[58] W.B. Zhang, D.P. McManus, Recent advances in the immunology and diagnosis of echinococcosis, FEMS Immunol. Med. Microbiol. 47 (2006) 24–41.